

# Neurons that Remember How We Got There

Walter Senn<sup>1,\*</sup> and Johanni Brea<sup>1</sup>

<sup>1</sup>Department of Physiology, University of Bern, Bühlplatz 5, 3012 Bern, Switzerland

\*Correspondence: [senn@pyl.unibe.ch](mailto:senn@pyl.unibe.ch)

<http://dx.doi.org/10.1016/j.neuron.2015.01.029>

In this issue of *Neuron*, [Daie et al. \(2015\)](#) show that the eye velocity-to-position neural integrator not only encodes the position, but also how it was reached. Representing content and context in the same neuronal population may form a general coding principle.

Those among us who go to work alternatively by bike or by bus will know the situation: when in the evening on the way home the crumbling feeling creeps over that something doesn't fit—then you realize in the bus that you have forgotten the bike with which you left in the morning for work. We may console ourselves by our focused concentration and, after all, being in the office by itself doesn't yet remind us how we got there. But now, [Daie et al. \(2015\)](#) explain that the same neuronal population that codes for a position also keeps the memory of how this position was reached. It just needs to be properly read out and be separated from the positional information.

The neuronal population that is the subject of the study is the oculomotor velocity-to-position neural integrator (VPNI) in the behaving zebrafish larvae, which also has its homolog in primates ([Joshua and Lisberger, 2014](#)). It is involved in the horizontal movement of the eyes and in keeping their position. Anatomically, the population in the zebrafish consists of roughly 100 bilaterally distributed medullary neurons in the inferior reticular formation. These position neurons receive saccadic, visual, and vestibular afferents and project to multiple targets such as the eye oculomotor nuclei, the cerebellum, and the thalamus. The neurons are shown to integrate (in the sense of calculus) afferent signals in time such that “velocity-encoding” presynaptic bursts move the “position-encoding” VPNI average firing rate to another level where it stays without further input ([Aksay et al., 2001](#)). Crucially, the same average firing rate and hence the same eye position can be reached in two different behavioral paradigms: by either a short spontaneous saccade of roughly 200-ms duration, or by a slow pursuit

movement tracking an optokinetic stimulus that stops at the target position.

[Daie et al. \(2015\)](#) were recording the neuronal activities of the VPNI neurons by two-photon calcium imaging during and after a saccade or an optokinetic pursuit of the eye to the same position. They found that the spatial distribution of activity and its persistence differed across the neurons in the two movement-inducing paradigms. While a differentiation is expected due to the unequal driving signals in the pre-fixation period, this differentiation remained even during the fixation period where the eye position and the VPNI average firing rate were the same. During fixation, the eyes still showed a small drift, and hence the VPNI is not a perfect integrator. The average activity decay was in both paradigms on a scale of roughly 7 s, and previous work revealed a spatial gradient of decay times of the individual neurons across the VPNI population ([Miri et al., 2011](#)). The striking new finding is that this spatial gradient is just opposite in the two movement-inducing paradigms. After a saccade, more caudally located neurons tended to be more persistent than the rostral neurons, and after the optokinetic induction, the reversed pattern was observed with more persistent neurons being located rostrally. This finding suggests that VPNI encodes the context by the spatial activity pattern, in addition to representing the position by the average firing rate.

To understand how a recurrent neural network can simultaneously encode position and context we consider the dynamics of the recurrent network formed by the VPNI. Previous work was suggesting a line attractor network that integrates inputs and keeps the activity level in the absence of input with the help of reverberating recurrent input ([Seung, 1996; Gold-](#)

[man et al., 2009](#)). Such attractor networks are described by the activity vector  $r(t)$  that changes due to the neuronal leak, the recurrent input, and the external input

$$\tau_{neur} \frac{dr}{dt} = -r + Wr + I, \quad (\text{Equation 1})$$

with  $\tau_{neur}$  representing the neuronal time constant,  $W$  the recurrent connectivity matrix, and  $I(t)$  a time-dependent velocity input to the individual neurons. The recurrent input in the line attractor model stabilizes all activity patterns  $r$  proportional to a “mode”  $J$ , where the mode  $J$  is characterized by the relative firing rates of the neurons in the network. Input that is co-aligned with this mode changes the average firing rate, but leaves the spatial pattern unchanged. The average firing rate (e.g., position) thus represents the integrated input (e.g., velocity signal). Formally, we set the recurrent connections  $W = JJ^T$ , where mode  $J$  has unit length, i.e.,  $J^T J = 1$ . Therefore  $WJ = J$ , and each rate vector on the line  $r = sJ$  satisfies  $-r + Wr = 0$ . The network then becomes a pure integrator since solving [Equation 1](#) for  $r$  yields

$$r(t) = \frac{1}{\tau_{neur}} \int dt' I(t'). \quad (\text{Equation 2})$$

More sophisticated neuronal transfer functions than the linear one in [Equation 1](#) could be considered ([Fisher et al., 2013](#)), but it is remarkable that this simple model yields a very good description of recorded neuronal activity.

By requiring that at any time the rate  $r(t)$  is co-aligned with the mode  $J$ , we implicitly impose this property also on the input,  $I \propto J$  (see [Equation 2](#)). Any component of the input  $I$  orthogonal to mode  $J$  would decay with time constant  $\tau_{neur}$ . But the experimental paradigm considered by

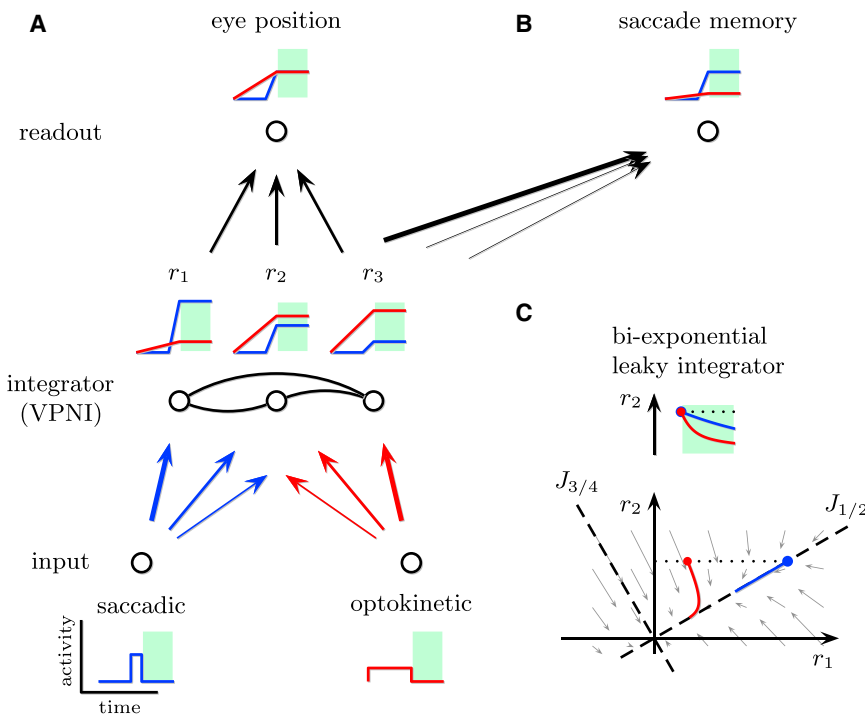


**Figure 1. A Multi-Modal VPNI for Horizontal Eye Movements in the Zebrafish**

(A) The same eye position is encoded in the average population firing rate upon fast saccadic or slow optokinetic velocity input.  
 (B) The identity of the stimulus (here a saccade) can still be read out in the post-stimulus interval (light green).  
 (C) The same VPNI neuron can display different activity decays depending on how the preceding input pattern decomposes into slow ( $J_{1/2}$ ) or fast ( $J_{3/4}$ ) activity modes.

Daie and colleagues has two types of input, a saccadic and an optokinetic input, and their recordings show that the two different inputs lead to two different spatial activity patterns that both show persistent activity. To describe this behavior, the line attractor must be extended to a “plane attractor” with a plane spanned up by two (orthonormal) modes  $J_1$  and  $J_2$ , and with a saccadic input  $I_{sacc} = s_1J_1 + s_2J_2$  and optokinetic input  $I_{okr} = o_1J_1 + o_2J_2$  within that plane. These different inputs are symbolized in Figure 1A, bottom, by the blue arrows representing the shorter, but stronger, saccadic input that dominates our left (“caudal”) VPNI, and by the red arrows representing the optokinetic input that dominates the right (“rostral”) VPNI. The persistent activity after applying either of the inputs is represented by the stationary firing rates of the three VPNI neurons (Figure 1A, middle, light green). A connectivity matrix forming a plane attractor is  $=J_1J_1^T + J_2J_2^T$ , since for this choice

$WJ_1 = J_1$  and also  $WJ_2 = J_2$ . As required by the behavioral paradigm, the total firing rate is the same after the saccadic and optokinetic input, and hence both inputs lead to the same position (shown in the “eye position” readout of Figure 1A, top). But saccadic and optokinetic input lead to a different spatial activity pattern, which thus can be said to encode the context. This stands in contrast to the line attractor, where the spatial activity pattern does not encode anything particular. Therefore it is now also possible to read out the identity of the afferent velocity signal: another linear combination of the VPNI activities yields a positive response if the saccadic input was present, and almost no response if the optokinetic input was present (Figure 1B).

Memory retention times in general must be adapted to the behavioral scale (Brea et al., 2014), and so does the zebrafish VPNI leak on a rough time scale of  $\tau_{slow} = 7s$ . In the model this can be accounted for by setting

$W = \lambda_{slow}(J_1J_1^T + J_2J_2^T)$  with  $\lambda_{slow} = 0.99$ . This results in a small leak term  $-r + Wr = -(1 - \lambda_{slow})r$  in Equation 1, and hence in an effective decay time constant  $\tau_{slow} = \tau_{neur}/(1 - \lambda_{slow})$  of the network that is 100 times slower than the neuronal time constant. Since the data reveal different decay times for the various VPNI neurons, additional faster ( $\sim 2$  s) decaying modes  $J_3$  and  $J_4$  have been extracted (with  $\lambda_{fast} \approx 0.9$ ). The final connection matrix, correspondingly, is the sum of four terms. When mimicking the saccadic velocity signal with a brief input  $I_{sacc} = s_1J_1 + s_3J_3$ , say of duration  $\tau_{neur}$ , the post-saccadic activation pattern becomes

$$r_{sacc}(t) = s_1J_1e^{-t/\tau_{slow}} + s_3J_3e^{-t/\tau_{fast}} \quad (\text{Equation 3})$$

with some “singular values”  $s_1$  and  $s_2$  also extracted from the data. Similarly, the post-optokinetic activation pattern  $r_{okr}(t)$  is composed of the modes  $J_1$ ,  $J_2$ , and  $J_4$ , and displays also a bi-exponential decay. An example of the activity decay for the same neuron during the post-saccadic and post-optokinetic period is shown in Figure 1C, together with trajectories of  $r_{sacc}$  and  $r_{okr}$  restricted to the first two neurons. In the data, the single-exponential decay times fitted to the individual neurons in the post-saccadic and post-optokinetic fixation period show reversed spatial gradients, similarly to the activity distribution in Figure 1A (middle).

The eye VPNI of the zebrafish larvae is a paradigmatic example of a closed sensory-to-motor loop of which we begin to have a functional understanding. It would be exciting to build a one-to-one neuronal model in silico that is based on connectomics data (Ahrens et al., 2012) and detailed neuron modeling (Fisher et al., 2013), and that reproduces the known and new functionalities yet to be discovered. For instance, the described VPNI neurons that are driven by saccadic input may activate fast-twitch and non-twitch motor units in a specific recruitment order (Mendell, 2005), and the observed overshoot of the eye movement may be corrected by a delayed activation of antagonistic eye muscles. Yet, the observation of a simultaneous encoding of position and input signal that led to this position may point to a more general population coding principle. Multiple dimensions of

a percept or a memory could be encoded in the same population such as motion or color, and the dimension that is read out may change with the task (Mante et al., 2013). Combining different claims using Bayesian inference further requires the representation of each claim together with its evidence, where the evidence depends on the context (Pouget et al., 2013). For instance, the evidence we attribute to the claim “VPNI is a multi-modal integrator” depends on the experiments supporting this claim, and this contextual information may be jointly encoded with the claim itself. Daie et al. (2015), with their publication in *Neuron*, clearly increase the evidence that the encoding of content and

context for horizontal eye movements in zebrafish is tightly entangled in a small neuronal population in the brain stem.

#### REFERENCES

- Ahrens, M.B., Li, J.M., Orger, M.B., Robson, D.N., Schier, A.F., Engert, F., and Portugues, R. (2012). *Nature* 485, 471–477.
- Aksay, E., Gamkrelidze, G., Seung, H.S., Baker, R., and Tank, D.W. (2001). *Nat. Neurosci.* 4, 184–193.
- Brea, J., Urbanczik, R., and Senn, W. (2014). *PLoS Comput. Biol.* 10, e1003640.
- Daie, K., Goldman, M.S., and Aksay, E.R.F. (2015). *Neuron* 85, this issue, 847–860.
- Fisher, D., Olasagasti, I., Tank, D.W., Aksay, E.R., and Goldman, M.S. (2013). *Neuron* 79, 987–1000.
- Goldman, M., Compte, A., and Wang, X. (2009). In *Encyclopedia of Neuroscience, Volume 6*, L. Squire, ed. (2009). (Academic Press), pp. 165–178.
- Joshua, M., and Lisberger, S.G. (2014). *Neuroscience*. Published online May 2, 2014. <http://dx.doi.org/10.1016/j.neuroscience.2014.04.048>.
- Mante, V., Sussillo, D., Shenoy, K.V., and Newsome, W.T. (2013). *Nature* 503, 78–84.
- Mendell, L.M. (2005). *J. Neurophysiol.* 93, 3024–3026.
- Miri, A., Daie, K., Arrenberg, A.B., Baier, H., Aksay, E., and Tank, D.W. (2011). *Nat. Neurosci.* 14, 1150–1159.
- Pouget, A., Beck, J.M., Ma, W.J., and Latham, P.E. (2013). *Nat. Neurosci.* 16, 1170–1178.
- Seung, H.S. (1996). *Proc. Natl. Acad. Sci. USA* 93, 13339–13344.